

RECENT DEVELOPMENTS IN LOW x PHYSICS ¹

J. Kwieciński

Department of Theoretical Physics

H. Niewodniczański Institute of Nuclear Physics

Kraków, Poland.

Abstract

The QCD expectations for the behaviour of the deep inelastic scattering structure functions in the region of small values of the Bjorken parameter x are summarized. The Balitzkij, Lipatov, Fadin, Kuraev (BFKL) equation which sums the leading powers of $\alpha_s \ln(1/x)$ is described and confronted with the "conventional" formalism based on the leading order QCD evolution equations. The small x behaviour of the spin dependent structure function g_1 is also discussed. The dedicated measurements of the hadronic final state in deep inelastic scattering at small x probing the QCD pomeron are described. This includes discussion of the deep inelastic scattering accompanied by forward jets as well as production of forward prompt photons and π^0 -s. Finally the basic facts concerning the deep inelastic diffraction are briefly summarized.

1. Introduction

The advent of the HERA ep collider has opened up a possibility to test QCD in the new and hitherto unexplored regime of the small values of the Bjorken parameter x . This parameter is, as usual, defined as $x = Q^2/(2pq)$ where p is the proton four momentum, q the four momentum transfer between the leptons and $Q^2 = -q^2$. Perturbative QCD predicts that several new phenomena will occur when the parameter x specifying the longitudinal momentum fraction of a hadron carried by a parton (i.e. by a quark or by a gluon) becomes very small [1, 2]. The main expectation is that the gluon densities should strongly grow in this limit, eventually leading to the parton saturation effects [1, 2, 3, 4]. The small x behaviour of the structure functions is driven by the gluon through the $g \rightarrow q\bar{q}$ transition and the increase of gluon distributions with decreasing x implies a similar increase of the deep inelastic lepton - proton scattering structure function F_2 as the Bjorken parameter x decreases [5]. The recent experimental data are consistent with this perturbative QCD prediction that the structure function $F_2(x, Q^2)$ should strongly grow with the decreasing Bjorken parameter x [6, 7, 8, 9, 10].

The purpose of these lectures is to summarize the QCD expectations for the small x behaviour of the deep inelastic scattering structure functions. After briefly reviewing predictions of the Regge theory we shall discuss the Balitzkij, Lipatov, Fadin, Kuraev (BFKL) [11, 12]

¹Based on lectures given at the XXXVIth Cracow School of Theoretical Physics, Zakopane, Poland, June 1996

equation which sums the leading powers of $\alpha_s \ln(1/x)$. We will also briefly describe the "conventional" formalism based on the leading (and next to leading) order QCD evolution equations and confront it with the BFKL equation. Besides the structure functions $F_2(x, Q^2)$ and $F_L(x, Q^2)$ we shall also consider the spin structure function $g_1(x, Q^2)$. The novel feature in the latter case is the appearance of the double logarithmic terms i.e. powers of $\alpha_s \ln^2(1/x)$ at each order of the perturbative expansion. Finally we will also discuss dedicated measurements of the final state in deep inelastic scattering which can probe the detailed dynamical content of the QCD pomeron.

2. Structure functions at low x

Small x behaviour of structure functions for fixed Q^2 reflects the high energy behaviour of the virtual Compton scattering total cross-section with increasing total CM energy squared W^2 since $W^2 = Q^2(1/x - 1)$. The appropriate framework for the theoretical description of this behaviour is the Regge pole exchange picture [13].

The high energy behaviour of the total hadronic and (real) photoproduction cross-sections can be economically described by two contributions: an (effective) pomeron with its intercept slightly above unity (~ 1.08) and the leading meson Regge trajectories with intercept $\alpha_R(0) \approx 0.5$ [14]. The reggeons can be identified as corresponding to ρ, ω, f or A_2 exchange(s) depending upon the quantum numbers involved. All these reggeons have approximately the same intercept. One refers to the pomeron obtained from the phenomenological analysis of hadronic total cross sections as the "soft" pomeron since the bulk of the processes building-up the cross sections are low p_t (soft) processes.

The Regge pole model gives the following parametrization of the deep inelastic scattering structure function $F_2(x, Q^2)$ at small x [15, 16]

$$F_2(x, Q^2) = \sum_i \tilde{\beta}_i(Q^2) x^{1-\alpha_i(0)}. \quad (1)$$

The relevant reggeons are those which can couple to two (virtual) photons. The (singlet) part of the structure function F_2 is controlled at small x by pomeron exchange, while the non-singlet part $F_2^{NS} = F_2^p - F_2^n$ by the A_2 reggeon. Neither pomeron nor A_2 reggeons couple to the spin structure function $g_1(x, Q^2)$ which is described at small x by the exchange of reggeons corresponding to axial vector mesons [16, 17] i.e. to A_1 exchange for the non-singlet part $g_1^{NS} = g_1^p - g_1^n$ etc.

$$g_1^{NS}(x, Q^2) = \gamma(Q^2) x^{-\alpha_{A_1}(0)}. \quad (2)$$

The reggeons which correspond to axial vector mesons are expected to have very low intercept (i.e. $\alpha_{A_1} \leq 0$ etc.).

The experimental results from HERA show that the proton structure function $F_2(x, Q^2)$ for moderate and large Q^2 values ($Q^2 > 1.5 \text{ GeV}^2$ or so) grows more rapidly than expected on the basis of the straightforward extension of the Regge pole parametrization with the relatively small intercept of the effective pomeron ($\alpha_P(0) \approx 1.08$) [10]. This result is consistent with perturbative QCD which predicts much stronger increase of the parton distributions and of the DIS structure functions with decreasing parameter x than that which would follow from equation (1) with $\alpha_P(0) \approx 1.08$. The high energy behaviour which follows from perturbative

QCD is often referred to as being related to the "hard" pomeron in contrast to the soft pomeron describing the high energy behaviour of hadronic and photoproduction cross-sections.

The relevant framework for discussing the pomeron in perturbative QCD and the small x limit of parton distributions is the leading $\ln 1/x$ (LL1/ x) approximation which corresponds to the sum of those terms in the perturbative expansion where the powers of α_s are accompanied by the leading powers of $\ln(1/x)$ [1, 2, 3, 4, 11, 12]. At small x the dominant role is played by the gluons and the quark (antiquark) distributions as well as the deep inelastic structure functions $F_{2,L}(x, Q^2)$ are also driven by the gluons through the $g \rightarrow q\bar{q}$ transitions. Dominance of gluons in high energy scattering follows from the fact that they carry spin equal to unity. The basic dynamical quantity at small x is the unintegrated gluon distribution $f(x, Q_t^2)$ where x denotes the momentum fraction of a parent hadron carried by a gluon and Q_t its transverse momentum. The unintegrated distribution $f(x, Q_t^2)$ is related in the following way to the more familiar scale dependent gluon distribution $g(x, Q^2)$:

$$xg(x, Q^2) = \int^{Q^2} \frac{dQ_t^2}{Q_t^2} f(x, Q_t^2). \quad (3)$$

In the leading $\ln(1/x)$ approximation the unintegrated distribution $f(x, Q_t^2)$ satisfies the BFKL equation [11, 12, 18] which has the following form:

$$f(x, Q_t^2) = f^0(x, Q_t^2) + \bar{\alpha}_s \int_x^1 \frac{dx'}{x'} \int \frac{d^2q}{\pi q^2} \left[\frac{Q_t^2}{(\mathbf{q} + \mathbf{Q}_t)^2} f(x', (\mathbf{q} + \mathbf{Q}_t)^2) - f(x', Q_t^2) \Theta(Q_t^2 - q^2) \right] \quad (4)$$

where

$$\bar{\alpha}_s = \frac{3\alpha_s}{\pi} \quad (5)$$

This equation sums the ladder diagrams with gluon exchange accompanied by virtual corrections which are responsible for the gluon reggeization. The first and the second terms on the right hand side of eq. (4) correspond to real gluon emission with q being the transverse momentum of the emitted gluon, and to the virtual corrections respectively. $f^0(x, Q_t^2)$ is a suitably defined inhomogeneous term.

For the fixed coupling case eq. (4) can be solved analytically and the leading behaviour of its solution at small x is given by the following expression:

$$f(x, Q_t^2) \sim (Q_t^2)^{\frac{1}{2}} \frac{x^{-\lambda_{BFKL}}}{\sqrt{\ln(\frac{1}{x})}} \exp\left(-\frac{\ln^2(Q_t^2/\bar{Q}^2)}{2\lambda'' \ln(1/x)}\right) \quad (6)$$

with

$$\lambda_{BFKL} = 4\ln(2)\bar{\alpha}_s \quad (7)$$

$$\lambda'' = \bar{\alpha}_s 28\zeta(3) \quad (8)$$

where the Riemann zeta function $\zeta(3) \approx 1.202$. The parameter \bar{Q} is of nonperturbative origin.

The quantity $1 + \lambda_{BFKL}$ is equal to the intercept of the so - called BFKL pomeron. Its potentially large magnitude (~ 1.5) should be contrasted with the intercept $\alpha_{soft} \approx 1.08$ of the (effective) "soft" pomeron which has been determined from the phenomenological analysis of

the high energy behaviour of hadronic and photoproduction total cross-sections [14].

The solution of the BFKL equation reflects its diffusion pattern which is the direct consequence of the absence of transverse momentum ordering along the gluon chain. The interrelation between the diffusion of transverse momenta towards both the infrared and ultraviolet regions **and** the increase of gluon distributions with decreasing x is a characteristic property of QCD at low x . It has important consequences for the structure of the hadronic final state in deep inelastic scattering at small x and this problem will be discussed with some detail in the next Section.

In practice one introduces the running coupling $\bar{\alpha}_s(Q_t^2)$ in the BFKL equation (4). This requires the introduction of an infrared cut-off to prevent entering the infrared region where the coupling becomes large. The effective intercept λ_{BFKL} found by numerically solving the equation depends on the magnitude of this cut-off [19]. The running coupling does also affect the diffusion pattern of the solution. The effective intercept λ_{BFKL} turns out to be also sensitive on the (formally non-leading) additional constraint $q^2 < Q_t^2 x'/x$ in the real emission term in eq. (4) which follows from the requirement that the virtuality of the last gluon in the chain is dominated by Q_t^2 [20, 21]. For fixed coupling $\bar{\alpha}_s$ the modified BFKL equation with the constraint $q^2 < Q_t^2 x'/x$ can be solved analytically since imposing this constraint still preserves the scale invariance of this equation. One can also derive the NLO formula for λ_{BFKL} which reads:

$$\lambda_{BFKL} = \bar{\alpha}_s 4 \ln 2 (1 - 4.15 \bar{\alpha}_s) \quad (9)$$

In Fig. 1 we show λ_{BFKL} plotted as a function of $\bar{\alpha}_s$. We also show the LO (7) and NLO (9) results. We see that the constraint $q^2 < Q_t^2 x'/x$ significantly affects the magnitude of λ_{BFKL} . It may also be seen that the pure NLO result may be unreliable even for values of $\bar{\alpha}_s \sim 0.1$.

The impact of the momentum cut-offs on the solution of the BFKL equation has also been discussed in refs. [22, 23]. In impact parameter representation the BFKL equation offers an interesting interpretation in terms of colour dipoles [24]. It should also be emphasised that the complete calculation of the next-to-leading corrections to the BFKL equation has recently become presented in ref. [25].

The structure functions $F_{2,L}(x, Q^2)$ are driven at small x by the gluons and are related in the following way to the unintegrated distribution f :

$$F_{2,L}(x, Q^2) = \int_x^1 \frac{dx'}{x'} \int \frac{dQ_t^2}{Q_t^2} F_{2,L}^{box}(x', Q_t^2, Q^2) f\left(\frac{x}{x'}, Q_t^2\right). \quad (10)$$

The functions $F_{2,L}^{box}(x', Q_t^2, Q^2)$ may be regarded as the structure functions of the off-shell gluons with virtuality Q_t^2 . They are described by the quark box (and crossed box) diagram contributions to the photon-gluon interaction. The small x behaviour of the structure functions reflects the small z ($z = x/x'$) behaviour of the gluon distribution $f(z, Q_t^2)$.

Equation (10) is an example of the " k_t factorization theorem" which relates measurable quantities (like DIS structure functions) to the convolution in both longitudinal as well as in transverse momenta of the universal gluon distribution $f(z, Q_t^2)$ with the cross-section (or structure function) describing the interaction of the "off-shell" gluon with the hard probe [26, 27, 28]. The k_t factorization theorem is the basic tool for calculating the observable quantities in the small x region in terms of the (unintegrated) gluon distribution f which is the solution of the BFKL equation.

The leading - twist part of the k_t factorization formula can be rewritten in a collinear factorization form. The leading small x effects are then automatically resummed in the splitting functions and in the coefficient functions. The k_t factorization theorem can in fact be used as the tool for calculating these quantities. Thus, for instance, the moment function $\bar{P}_{gg}(\omega, \alpha_s)$ of the splitting $P_{gg}(z, \alpha_s)$ function is represented in the following form (in the so called Q_0^2 regularization and DIS scheme [27]):

$$\bar{P}_{gg}(\omega, \alpha_s) = \frac{\gamma_{gg}^2\left(\frac{\bar{\alpha}_s}{\omega}\right)\tilde{F}_2^{box}\left(\omega=0, \gamma=\gamma_{gg}\left(\frac{\bar{\alpha}_s}{\omega}\right)\right)}{2\sum_i e_i^2} \quad (11)$$

where $\tilde{F}_2^{box}(\omega, \gamma)$ is the Mellin transform of the moment function $\bar{F}_2^{box}(\omega, Q_t^2, Q^2)$ i.e.

$$\bar{F}_2^{box}(\omega, Q_t^2, Q^2) = \frac{1}{2\pi i} \int_{1/2-i\infty}^{1/2+i\infty} d\gamma \tilde{F}_2^{box}(\omega, \gamma) \left(\frac{Q^2}{Q_t^2}\right)^\gamma \quad (12)$$

and the anomalous dimension $\gamma_{gg}\left(\frac{\bar{\alpha}_s}{\omega}\right)$ has the following expansion [29];

$$\gamma_{gg}\left(\frac{\bar{\alpha}_s}{\omega}\right) = \sum_{n=1}^{\infty} c_n \left(\frac{\bar{\alpha}_s}{\omega}\right)^n \quad (13)$$

This expansion gives the following expansion of the splitting function P_{gg}

$$zP_{gg}(z, \alpha_s) = \sum_1^{\infty} c_n \frac{[\alpha_s \ln(1/z)]^{n-1}}{(n-1)!} \quad (14)$$

Representation (11) generates the following expansion of the splitting function $P_{gg}(z, \alpha_s)$ at small z :

$$zP_{gg}(z, \alpha_s) = \frac{\alpha_s}{2\pi} zP^{(0)}(z) + (\bar{\alpha}_s)^2 \sum_{n=1}^{\infty} b_n \frac{[\bar{\alpha}_s \ln(1/z)]^{n-1}}{(n-1)!} \quad (15)$$

The first term on the right hand side of eq. (15) vanishes at $z = 0$. It should be noted that the splitting function P_{gg} is formally non-leading at small z when compared with the splitting function P_{gg} . For moderately small values of z however, when the first few terms in the expansions (13) and (15) dominate, the BFKL effects can be much more important in P_{gg} than in P_{gg} . This comes from the fact that in the expansion (15) all coefficients b_n are different from zero while in eq. (13) we have $c_2 = c_3 = 0$ [29]. The small x resummation effects within the conventional QCD evolution formalism have recently been discussed in refs. [30, 31, 32, 33, 34, 35]. One finds in general that at the moderately small values of x which are relevant for the HERA measurements, the small x resummation effects in the splitting function P_{gg} have a much stronger impact on F_2 than the small x resummation in the splitting function P_{gg} . This reflects the fact, which has already been mentioned above, that in the expansion (15) all coefficients b_n are different from zero while in eq. (13) we have $c_2 = c_3 = 0$. It should also be remembered that the BFKL effects in the splitting function $P_{gg}(z, \alpha_s)$ can significantly affect extraction of the gluon distribution out of the experimental data on the slope of the structure function $F_2(x, Q^2)$ which is based on the following relation:

$$Q^2 \frac{\partial F_2(x, Q^2)}{\partial Q^2} \simeq 2 \sum_i e_i^2 \int_x^1 dz P_{gg}(z, \alpha_s(Q^2)) \frac{x}{z} g\left(\frac{x}{z}, Q^2\right) \quad (16)$$

A more general treatment of the gluon ladder than that which follows from the BFKL formalism is provided by the Catani, Ciafaloni, Fiorani, Marchesini (CCFM) equation based on angular ordering along the gluon chain [36, 37, 38]. This equation embodies both the BFKL

equation at small x and the conventional Altarelli-Parisi evolution at large x . The unintegrated gluon distribution f now acquires dependence upon an additional scale Q which specifies the maximal angle of gluon emission. The CCFM equation has the following form :

$$f(x, Q_t^2, Q^2) = \hat{f}^0(x, Q_t^2, Q^2) + \bar{\alpha}_s \int_x^1 \frac{dx'}{x'} \int \frac{d^2q}{\pi q^2} \Theta(Q - qx/x') \Delta_R\left(\frac{x}{x'}, Q_t^2, q^2\right) \frac{Q_t^2}{(\mathbf{q} + \mathbf{Q}_t)^2} f(x', (\mathbf{q} + \mathbf{Q}_t)^2, q^2) \quad (17)$$

where the theta function $\Theta(Q - qx/x')$ reflects the angular ordering constraint on the emitted gluon. The "non-Sudakov" form-factor $\Delta_R(z, Q_t^2, q^2)$ is now given by the following formula:

$$\Delta_R(z, Q_t^2, q^2) = \exp \left[-\bar{\alpha}_s \int_z^1 \frac{dz'}{z'} \int \frac{dq'^2}{q'^2} \Theta(q'^2 - (qz')^2) \Theta(Q_t^2 - q'^2) \right] \quad (18)$$

Eq.(17) still contains only the singular term of the $g \rightarrow gg$ splitting function at small z . Its generalization which would include remaining parts of this vertex (as well as quarks) is possible. The numerical analysis of this equation was presented in ref. [37]. The CCFM equation which is the generalization of the BFKL equation generates the steep $x^{-\lambda}$ type of behaviour for the deep inelastic structure functions as the effect of the leading $\ln(1/x)$ resummation [39]. The slope λ turns out to be sensitive on the (formally non-leading) additional constraint $q^2 < Q_t^2 x'/x$ in eq. (17) which follows from the requirement that the virtuality of the last gluon in the chain is dominated by Q_t^2 [20, 21].

The HERA data can be described quite well using the BFKL and CCFM equations combined with the factorization formula (10) [21, 39]. One can however obtain satisfactory description of the HERA data staying within the scheme based on the Altarelli-Parisi equations alone without the small x resummation effects being included in the formalism [40, 41, 42]. In the latter case the singular small x behaviour of the gluon and sea quark distributions has to be introduced in the parametrization of the starting distributions at the moderately large reference scale $Q^2 = Q_0^2$ (i.e. $Q_0^2 \approx 4\text{GeV}^2$ or so) [40]. One can also generate steep behaviour dynamically starting from non-singular "valence-like" parton distributions at some very low scale $Q_0^2 = 0.35\text{GeV}^2$ [41]. In the latter case the gluon and sea quark distributions exhibit "double logarithmic behaviour" [43]

$$F_2(x, Q^2) \sim \exp \left(2\sqrt{\xi(Q^2, Q_0^2) \ln(1/x)} \right) \quad (19)$$

where

$$\xi(Q^2, Q_0^2) = \int_{Q_0^2}^{Q^2} \frac{dq^2}{q^2} \frac{3\alpha_s(q^2)}{\pi}. \quad (20)$$

For very small values of the scale Q_0^2 the evolution length $\xi(Q^2, Q_0^2)$ can become large for moderate and large values of Q^2 and the "double logarithmic" behaviour (19) is, within the limited region of x , similar to that corresponding to the power like increase of the type $x^{-\lambda}$, $\lambda \approx 0.3$. In Fig. 2 we summarize results of the recent QCD parton model analysis of the low x data from HERA and from the E665 experiment at Fermilab [42].

The discussion presented above concerned the small x behaviour of the singlet structure function which was driven by the gluon through the $g \rightarrow q\bar{q}$ transition. The gluons of course decouple from the non-singlet channel and the mechanism of generating the small x behaviour in this case is different.

The novel feature of the non-singlet channel is the appearance of the **double** logarithmic terms i.e. powers of $\alpha_s \ln^2(1/x)$ at each order of the perturbative expansion [44, 45, 46, 47, 48]. These double logarithmic terms are generated by the ladder diagrams with quark (antiquark) exchange along the chain. The ladder diagrams can acquire corrections from the "bremsstrahlung" contributions [46, 48] which do not vanish for the polarized structure function $g_1^{NS}(x, Q^2)$ [48]. They are however relatively unimportant and are non-leading in the $1/N_c$ expansion.

In the approximation where the leading double logarithmic terms are generated by ladder diagrams with quark (antiquark) exchange along the chain the unintegrated non-singlet spin dependent quark distribution $\Delta f_q^{NS}(x, k_t^2)$ ($\Delta f_q^{NS} = \Delta u + \Delta \bar{u} - \Delta d - \Delta \bar{d}$) satisfies the following integral equation :

$$\Delta f_q^{NS}(x, Q_t^2) = \Delta f_{q0}^{NS}(x, Q_t^2) + \tilde{\alpha}_s \int_x^1 \frac{dz}{z} \int_{Q_0^2}^{\frac{Q_t^2}{z}} \frac{dQ_t'^2}{Q_t'^2} \Delta f_q^{NS}\left(\frac{x}{z}, Q_t'^2\right) \quad (21)$$

where

$$\tilde{\alpha}_s = \frac{2}{3\pi} \alpha_s \quad (22)$$

and Q_0^2 is the infrared cut-off parameter. The upper limit Q_t^2/z in the integral equation (21) follows from the requirement that the virtuality of the quark at the end of the chain is dominated by Q_t^2 . A possible non-perturbative A_1 reggeon contribution has to be introduced in the driving term i.e.

$$\Delta f_{q0}^{NS}(x, Q_t^2) \sim x^{-\alpha_{A_1}(0)} \quad (23)$$

at small x .

Equation (21) implies the following equation for the moment function $\Delta \bar{f}_q^{NS}(\omega, Q_t^2)$

$$\Delta \bar{f}_q^{NS}(\omega, Q_t^2) = \Delta \bar{f}_{q0}^{NS}(\omega, Q_t^2) + \frac{\tilde{\alpha}_s}{\omega} \left[\int_{Q_0^2}^{Q_t^2} \frac{dQ_t'^2}{Q_t'^2} \Delta \bar{f}_q^{NS}(\omega, Q_t'^2) + \int_{Q_t^2}^{\infty} \frac{dQ_t'^2}{Q_t'^2} \left(\frac{Q_t^2}{Q_t'^2} \right)^\omega \Delta \bar{f}_q^{NS}(\omega, Q_t'^2) \right] \quad (24)$$

For fixed coupling $\tilde{\alpha}_s$ equation (24) can be solved analytically. Assuming for simplicity that the inhomogeneous term is independent of Q_t^2 (i.e. that $\Delta \bar{f}_{q0}^{NS}(\omega, Q_t^2) = C(\omega)$) we get the following solution of eq.(24):

$$\Delta \bar{f}_q^{NS}(\omega, Q_t^2) = C(\omega) R(\tilde{\alpha}_s, \omega) \left(\frac{Q_t^2}{Q_0^2} \right)^{\gamma^-(\tilde{\alpha}_s, \omega)} \quad (25)$$

where

$$\gamma^-(\tilde{\alpha}_s, \omega) = \frac{\omega - \sqrt{\omega^2 - 4\tilde{\alpha}_s}}{2} \quad (26)$$

and

$$R(\tilde{\alpha}_s, \omega) = \frac{\omega \gamma^-(\tilde{\alpha}_s, \omega)}{\tilde{\alpha}_s}. \quad (27)$$

Equation (26) defines the anomalous dimension of the moment of the non-singlet quark distribution in which the double logarithmic $\ln(1/x)$ terms i.e. the powers of $\frac{\alpha_s}{\omega^2}$ have been resummed to all orders. It can be seen from (26) that this anomalous dimension has a (square root) branch point singularity at $\omega = \bar{\omega}$ where

$$\bar{\omega} = 2\sqrt{\tilde{\alpha}_s}. \quad (28)$$

This singularity will of course be also present in the moment function $\Delta \bar{f}_q^{NS}(\omega, Q_t^2)$ itself. It should be noted that in contrast to the BFKL singularity whose position above unity was proportional to α_s , $\bar{\omega}$ is proportional to $\sqrt{\alpha_s}$ - this being the straightforward consequence of the fact that equation (24) sums double logarithmic terms $(\frac{\alpha_s}{\omega^2})^n$. This singularity gives the following contribution to the non-singlet quark distribution $\Delta f_q^{NS}(x, Q_t^2)$ at small x :

$$\Delta f_q^{NS}(x, Q_t^2) \sim \frac{x^{-\bar{\omega}}}{\ln^{3/2}(1/x)}. \quad (29)$$

The introduction of the running coupling effects in equation (24) turns the branch point singularity into the series of poles which accumulate at $\omega = 0$ [45]. The numerical analysis of the corresponding integral equation, with the running coupling effects taken into account, gives an effective slope ,

$$\lambda(x, Q_t^2) = \frac{d \ln \Delta f_q^{NS}(x, Q_t^2)}{d \ln(1/x)} \quad (30)$$

with magnitude $\lambda(x, Q_t^2) \approx 0.2 - 0.3$ at small x [49]. The result of this estimate suggests that a reasonable extrapolation of the (non-singlet) polarized quark densities would be to assume an $x^{-\lambda}$ behaviour with $\lambda \approx 0.2 - 0.3$. Similar extrapolations of the spin-dependent quark distributions towards the small x region have been assumed in several recent parametrizations of parton densities [50, 51, 52, 53]. The perturbative QCD effects become significantly amplified for the singlet spin structure function due to mixing with the gluons. The simple ladder equation may not however be applicable for an accurate description of the double logarithmic terms in the polarized gluon distribution ΔG [54]. The small x behaviour of the spin dependent structure function g_1 has also been discussed in refs. [55, 56].

3. Dedicated measurements probing the QCD pomeron in deep inelastic scattering at low x

It is expected that absence of transverse momentum ordering along the gluon chain which leads to the correlation between the increase of the structure function with decreasing x and the diffusion of transverse momentum should reflect itself in the behaviour of less inclusive quantities than the structure function $F_2(x, Q^2)$. The dedicated measurements of the low x physics which are particularly sensitive to this correlation are the deep inelastic scattering plus energetic forward jet events [57, 58, 59, 60, 61, 62], transverse energy flow in deep inelastic scattering [63, 64], production of jets separated by the large rapidity gap [65, 66] and dijet production in photoproduction [67] and in deep inelastic scattering [68]. Complementary measurement to deep inelastic scattering plus forward jet is the deep inelastic scattering accompanied by the forward prompt photon or forward prompt π^0 [69, 70].

In principle deep inelastic lepton scattering containing a measured energetic jet can provide a very clear test of the BFKL dynamics at low x [57, 58, 59, 60, 61, 62]. The idea is to study deep inelastic (x, Q^2) events which contain an identified jet (x_j, k_{Tj}^2) where $x \ll x_j$ and $Q^2 \approx k_{Tj}^2$. Since we choose events with $Q^2 \approx k_{Tj}^2$ the leading order QCD evolution (from k_{Tj}^2 to Q^2) is neutralized and attention is focussed on the small x , or rather small x/x_j behaviour. The small x/x_j behaviour of jet production is generated by the gluon radiation. Choosing the configuration $Q^2 \approx k_{Tj}^2$ we eliminate by definition gluon emission which corresponds to strongly ordered transverse momenta i.e. that emission which is responsible for the LO QCD evolution.

The measurement of jet production in this configuration may therefore test more directly the $(x/x_j)^{-\lambda}$ behaviour which is generated by the BFKL equation where the transverse momenta are not ordered.

The differential cross section for the deep inelastic + jet process depicted in Fig. 3a is given by [19]

$$\frac{\partial\sigma_j}{\partial x\partial Q^2} = \int dx_j \int dk_{jT}^2 \frac{4\pi\alpha^2}{xQ^4} \left[(1-y) \frac{\partial F_2}{\partial x_j \partial k_{jT}^2} + \frac{1}{2} y^2 \frac{\partial(2xF_T)}{\partial x_j \partial k_{jT}^2} \right] \quad (31)$$

where the differential structure functions have the following form

$$\frac{\partial^2 F_i}{\partial x_j \partial k_{jT}^2} = \frac{3\alpha_S(k_{jT}^2)}{\pi k_{jT}^4} \sum_a f_a(x_j, k_{jT}^2) \Phi_i\left(\frac{x}{x_j}, k_{jT}^2, Q^2\right) \quad (32)$$

for $i = T, L$. Assuming t -channel pole dominance the sum over the parton distributions is given by

$$\sum_a f_a = g + \frac{4}{9}(q + \bar{q}). \quad (33)$$

Recall that these parton distributions are to be evaluated at (x_j, k_{jT}^2) where they are well-known from the global analyses, so there are no ambiguities arising from a non-perturbative input.

The functions $\Phi_i(x/x_j, k_{jT}^2, Q^2)$ in (32) describe the virtual γ + virtual gluon fusion process including the ladder formed from the gluon chain of Fig. 3a. They can be obtained by solving the BFKL equation

$$\begin{aligned} \Phi_i(z, k_T^2, Q^2) &= \Phi_i^{(0)}(z, k_T^2, Q^2) + \\ \bar{\alpha}_s \int_z^1 \frac{dz'}{z'} \int \frac{d^2q}{\pi q^2} &\left[\frac{k_T^2}{(\mathbf{q} + \mathbf{k}_T)^2} \Phi_i(z', (\mathbf{q} + \mathbf{k}_T)^2, Q^2) - \Phi_i(z', k_T^2, Q^2) \Theta(k_T^2 - q^2) \right] \end{aligned} \quad (34)$$

The inhomogeneous or driving terms $\Phi_i^{(0)}$ correspond to the sum of the quark box and crossed-box contributions. For small z we have

$$\Phi_i^{(0)}(z, k_T^2, Q^2) \approx \Phi_i^{(0)}(z=0, k_T^2, Q^2) \equiv \Phi_i^{(0)}(k_T^2, Q^2). \quad (35)$$

We evaluate the $\Phi_i^{(0)}$ by expanding the four momentum in terms of the basic light-like four momenta p and $q' \equiv q + xp$. For example, the quark momentum κ in the box (see Fig. 3a) has the Sudakov decomposition

$$\kappa = \alpha p - \beta q' + \boldsymbol{\kappa}_T.$$

We carry out the integration over the box diagrams, subject to the quark mass-shell constraints, and find

$$\begin{aligned} \Phi_T^{(0)}(k_T^2, Q^2) &= 2 \sum_q e_q^2 \frac{Q^2}{4\pi^2} \alpha_S \int_0^1 d\beta \int d^2\kappa_T [\beta^2 + (1-\beta)^2] \left(\frac{\kappa_T^2}{D_1^2} - \frac{\boldsymbol{\kappa}_T \cdot (\boldsymbol{\kappa}_T - \mathbf{k}_T)}{D_1 D_2} \right) \\ \Phi_L^{(0)}(k_T^2, Q^2) &= 2 \sum_q e_q^2 \frac{Q^4}{\pi^2} \alpha_S \int_0^1 d\beta \int d^2\kappa_T \beta^2 (1-\beta)^2 \left(\frac{1}{D_1^2} - \frac{1}{D_1 D_2} \right). \end{aligned} \quad (36)$$

where the denominators D_i are of the form

$$\begin{aligned} D_1 &= \kappa_T^2 + \beta(1-\beta) Q^2 \\ D_2 &= (\boldsymbol{\kappa}_T - \mathbf{k}_T)^2 + \beta(1-\beta) Q^2, \end{aligned} \quad (37)$$

assuming massless quarks.

If the QCD coupling α_S is fixed we can solve the BFKL equation (34) and obtain an analytic expression for the leading small z behaviour of the solution, including its normalisation. Omitting the Gaussian diffusion factor in $\ln(k_T^2/Q^2)$ we find

$$\begin{aligned}\Phi_T(z, k_T^2, Q^2) &= \frac{9\pi^2}{512} \frac{2 \sum e_q^2 \alpha_S^{\frac{1}{2}}}{\sqrt{21\zeta(3)/2}} (k_T^2 Q^2)^{\frac{1}{2}} \frac{z^{-\lambda_{BFKL}}}{\sqrt{\ln(1/z)}} \left[1 + \mathcal{O}\left(\frac{1}{\ln(1/z)}\right) \right] \\ \Phi_L(z, k_T^2, Q^2) &= \frac{2}{9} \Phi_T(z, k_T^2, Q^2)\end{aligned}\tag{38}$$

Singular small z behaviour of the functions Φ_i leads to increase of the cross section for forward jet production with decreasing x . Recent H1 results concerning deep inelastic plus jet events are consistent with this prediction [61, 62].

As it has been mentioned above a complementary measurement to deep inelastic scattering plus forward jet is the deep inelastic scattering accompanied by the forward prompt photon or forward prompt π^0 [69, 70].

The prompt photon production in deep-inelastic scattering at small x is the process

$$“\gamma” + p \rightarrow \gamma(x_\gamma, k_{\gamma T}) + X,\tag{39}$$

sketched in Fig. 3b, in which the photon is identified in the final state. Deep inelastic events with small x and large x_γ offer an opportunity to identify the effects of the BFKL resummation of the $\alpha_S \ln(x_\gamma/x)$ contributions, which arise from the sum over the real and virtual gluon emissions, such as the one depicted in Fig. 3b. In analogy to the DIS + jet process, the advantage of process (39) is that the outgoing photon acts as a trigger to select events in which the deep-inelastic scattering occurs off a quark in a kinematic region where its distribution, $q(x_q, k_{\gamma T}^2)$, is known.

The differential structure functions for this process may be written in the form

$$\frac{\partial^2 F_i}{\partial x_\gamma \partial k_{\gamma T}^2} = \int \frac{d^2 k_{gT}}{\pi k_{gT}^4} \int \frac{dx_q}{x_q} \Phi_i\left(\frac{x}{x_q}, k_{gT}^2, Q^2\right) \sum_q e_q^2 [q(x_q, k_{\gamma T}^2) + \bar{q}(x_q, k_{\gamma T}^2)] \frac{|\mathcal{M}|^2}{z_\gamma z'_q}\tag{40}$$

for $i = T, L$. The variables are indicated on Fig. 3b and are defined below. The subprocess $q(k_q) + g(k_g) \rightarrow q(k'_q) + \gamma(k_\gamma)$ (and also $\bar{q}g \rightarrow \bar{q}\gamma$) is described by the two Feynman diagrams shown in Fig. 4. It has matrix element squared

$$|\mathcal{M}|^2 = 2 C_2(F) \frac{\alpha_S(k_{\gamma T}^2)}{2\pi} \frac{\alpha}{2\pi} \frac{k_{gT}^2 [1 + (1 - z_\gamma)^2]}{\hat{s}(-\hat{u})}\tag{41}$$

where $C_2(F) = 4/3$ and the invariants \hat{s} and \hat{u} are

$$\hat{s} = (k_\gamma + k'_q)^2, \quad \hat{u} = (k_q - k_\gamma)^2.\tag{42}$$

The fractional momenta x_i in (40) are defined by the Sudakov decomposition of the particle 4-momenta

$$k_i = x_i p' + \beta_i q' + \mathbf{k}_{iT}\tag{43}$$

The variables z_i in (40) and (41) are given by

$$z_i = x_i/x_q. \quad (44)$$

The 4-momenta of the outgoing photon and quark jet satisfy the on-mass-shell condition $k_i^2 = 0$ which gives

$$\beta_i = \frac{x}{x_i} \frac{k_{iT}^2}{Q^2} \quad (45)$$

for $i = \gamma$ or the outgoing quark q' .

In Fig. 5 we show the integrated cross section for prompt forward photon production as a function of x for three different Q^2 bins: 20-30, 30-40 and 40-50 GeV² respectively. The cross-section was calculated imposing various acceptance cuts. We compare the predictions for the case where the BFKL small x resummation is incorporated with those where the gluon radiation is neglected. The x dependence of the cross section is driven by the small z behaviour of the Φ_i . The results show a strong enhanced increase with decreasing x which is characteristic of the effect of soft gluon resummation.

In order to calculate the cross section for DIS + π^0 production (see Fig. 6) we have to convolute the DIS + jet cross section with the π^0 fragmentation functions. We obtain

$$\frac{\partial\sigma_\pi}{\partial x_\pi \partial k_{\pi T}} = \int_{x_\pi}^1 dz \int dx_j \int dk_{jT}^2 \left[\frac{\partial\sigma_g}{\partial x_j \partial k_{jT}^2} D_g^{\pi^0}(z, k_{\pi T}^2) + \sum_q \left(\frac{\partial\sigma_q}{\partial x_j \partial k_{jT}^2} D_q^{\pi^0}(z, k_{\pi T}^2) \right) \right] \times \\ \times \delta(x_\pi - zx_j) \delta(k_{\pi T} - zk_{jT}) \quad (46)$$

where the sum over q runs over all quark and antiquark flavours. The partonic differential cross sections can be obtained from (31) and (32) by substituting for the sum over the parton distributions $\sum_a f_a$ either the gluon distribution g or the quark or antiquark distribution $\frac{4}{9}q$ or $\frac{4}{9}\bar{q}$ respectively.

The results for the integrated cross-section for forward π^0 production in deep inelastic scattering are summarized in Fig. 7.

Conceptually similar process to deep inelastic scattering plus forward jet is that of the two-jet production separated by a large rapidity gap Δy in hadronic collisions or in photoproduction [65, 66]. Besides the characteristic $exp(\lambda\Delta y)$ dependence of the two-jet cross-section one expects significant weakening of the azimuthal back-to-back correlations of the two jets. This is the direct consequence of the absence of transverse momentum ordering along the gluon chain. Another measurement which should be sensitive to the QCD dynamics at small x is that of the transverse energy flow in deep inelastic lepton scattering in the central region away from the current jet and from the proton remnant [63]. The BFKL dynamics predicts in this case a substantial amount of transverse energy which should increase with decreasing x . The experimental data are consistent with this theoretical expectation [64]. Absence of transverse momentum ordering also implies weakening of the back-to-back azimuthal correlation of dijets produced close to the photon fragmentation region [67, 68].

Interesting insight into the BFKL equation (4) can also be obtained by studying the exclusive intermediate states of the gluon ladder which contains the multijet structure [71]. Jet structure is embodied in the BFKL equation via real gluon emission from the gluon chain prior

to its interaction with the photon probe (which takes place through the usual fusion subprocess $\gamma g \rightarrow q\bar{q}$). An observed jet is defined by a resolution parameter μ which specifies the minimum transverse momentum that must be carried by the emitted gluon for it to be detected. For realistic observed jets in the experiments at HERA, the lowest reasonable choice for the resolution cut-off parameter μ appears to be about $\mu = 3.5$ GeV. If an emitted gluon has transverse momentum $q_T < \mu$ then the radiation is said to be unresolved. The unresolved radiation must be treated at the same level as the virtual corrections to ensure that the singularities as $q_T^2 \rightarrow 0$ cancel in the q_T^2 integration. To do this we first rewrite the BFKL equation (4) in the symbolic form

$$f = f^{(0)} + \int_0^y dy' K \otimes f(y'), \quad (47)$$

where \otimes denotes the convolution over q and $y = \ln(1/x)$. We divide the real gluon emission contribution into resolved and unresolved parts using the identity

$$\Theta(q^2 - \mu^2) + \Theta(\mu^2 - q^2) = 1, \quad (48)$$

where the first term denotes the real resolved emission and the second the real unresolved emission. We then combine the unresolved component with the virtual contribution. That is

$$f = f^{(0)} + \int_0^y dy' (K_R + K_{UV}) \otimes f(y'), \quad (49)$$

where the kernel K_R for the *resolved* emissions with $q > \mu$ is given by

$$K_R \otimes f(y') = \bar{\alpha}_S(Q_t^2) Q_t^2 \int \frac{d^2q}{\pi q^2} \Theta(q^2 - \mu^2) \frac{1}{Q_t^2} f(y', Q_t^2), \quad (50)$$

while K_{UV} , the combined *unresolved* and *virtual* part of the kernel, satisfies

$$K_{UV} \otimes f(y') = \bar{\alpha}_S(Q_t^2) \int \frac{d^2q}{\pi q^2} \left[\frac{Q_t^2}{Q_t^2} f(y', Q_t^2) \Theta(\mu^2 - q^2) - f(y', Q_t^2) \Theta(Q_t^2 - q^2) \right], \quad (51)$$

with $Q_t^2 \equiv |\mathbf{q} + \mathbf{Q}_t|^2$. After resumming the unresolvable real emission and virtual correction terms the BFKL equation can be rearranged into the following form:

$$f(y) = \hat{f}^{(0)}(y) + \int_0^y dy' \hat{K} \otimes f(y') \quad (52)$$

where the driving term has become

$$\hat{f}^{(0)}(y) = \int_0^y dy' e^{(y-y')K_{UV}} \otimes \frac{\partial f^{(0)}}{\partial y'} \quad (53)$$

and the new kernel

$$\hat{K} = e^{(y-y')K_{UV}} \otimes K_R. \quad (54)$$

Iteration of the equation (52) generates decomposition of the unintegrated distribution f into the sum of contributions with different numbers of *resolved* gluon jets. That is

$$f(y) = \hat{f}^{(0)}(y) + \sum_{n=1}^{\infty} f^n(y) \quad (55)$$

where

$$f^1(y) = \int_0^y dy' \hat{K} \otimes \hat{f}^{(0)}(y')$$

and

$$f^n(y) = \int_0^y dy' \hat{K} \otimes f^{n-1}(y') \quad (56)$$

for $n > 1$. Using the k_t factorisation theorem (10) we get the contributions of different numbers of resolved jets to the structure functions which are illustrated in Fig.8.

4. Deep inelastic diffraction

Important process which is sensitive to the small x dynamics is the deep inelastic diffraction [72, 73]. Deep inelastic diffraction in ep inelastic scattering is a process:

$$e(p_e) + p(p) \rightarrow e'(p'_e) + X + p'(p') \quad (57)$$

where there is a large rapidity gap between the recoil proton (or excited proton) and the hadronic system X . To be precise process (57) reflects the diffractive dissociation of the virtual photon. Diffractive dissociation is described by the following kinematical variables:

$$\beta = \frac{Q^2}{2(p - p')q} \quad (58)$$

$$x_P = \frac{x}{\beta} \quad (59)$$

$$t = (p - p')^2. \quad (60)$$

Assuming that diffraction dissociation is dominated by the pomeron exchange and that the pomeron is described by a Regge pole one gets the following factorizable expression for the diffractive structure function [74, 75, 76, 78, 77]:

$$\frac{\partial F_2^{diff}}{\partial x_P \partial t} = f(x_P, t) F_2^P(\beta, Q^2, t) \quad (61)$$

where the "flux factor" $f(x_P, t)$ is given by the following formula :

$$f(x_P, t) = N \frac{B^2(t)}{16\pi} x_P^{1-2\alpha_P(t)} \quad (62)$$

with $B(t)$ describing the pomeron coupling to a proton and N being the normalisation factor. The function $F_2^P(\beta, Q^2, t)$ is the pomeron structure function which in the (QCD improved) parton model is related in a standard way to the quark and antiquark distribution functions in a pomeron.

$$F_2^P(\beta, Q^2, t) = \beta \sum e_i^2 [q_i^P(\beta, Q^2, t) + \bar{q}_i^P(\beta, Q^2, t)] \quad (63)$$

with $q_i^P(\beta, Q^2, t) = \bar{q}_i^P(\beta, Q^2, t)$. The variable β which is the Bjorken scaling variable appropriate for deep inelastic lepton-pomeron "scattering", has the meaning of the momentum fraction of the pomeron carried by the probed quark (antiquark). The quark distributions in a pomeron are assumed to obey the standard Altarelli-Parisi evolution equations:

$$Q^2 \frac{\partial q^P}{\partial Q^2} = P_{qq} \otimes q^P + P_{qg} \otimes g^P \quad (64)$$

with a similar equation for the evolution of the gluon distribution in a pomeron. The first term on the right hand side of the eq. (64) becomes negative at large β , while the second term remains positive and is usually very small at large β unless the gluon distributions are large and have a hard spectrum.

The data suggest that the slope of F_2^P as the function of Q^2 does not change sign even at relatively large values of β . This favours the hard gluon spectrum in a pomeron [79, 80], and should be contrasted with the behaviour of the structure function of the proton which, at large x , decreases with increasing Q^2 . The data on inclusive diffractive production favour

the soft pomeron with relatively low intercept. The diffractive production of vector mesons seems to require a "hard" pomeron contribution [10]. It has also been pointed out that the factorization property (61) may not hold in models based entirely on perturbative QCD when the pomeron is represented by the BFKL ladder [81, 82]. The factorization does not also hold when the exchange of the secondary Regge poles besides pomeron becomes important [83, 84]. The contribution of secondary Reggeons is expected to be significant at moderately small x_P and small values of β . The recent HERA results show violation of factorization in this region [84]. Finally let us point out that there exist also models of deep inelastic diffraction which do not rely on the pomeron exchange picture [85, 86].

4. Summary and conclusions

Perturbative QCD predicts indefinite increase of gluon distributions with decreasing x which generates similar increase of the structure functions through the $g \rightarrow q\bar{q}$ transitions. The indefinite growth of parton distributions cannot go on forever and has to be eventually stopped by parton screening which leads to the parton saturation. Most probably however the saturation limit is still irrelevant for the small x region which is now being probed at HERA. Besides discussing the theoretical and phenomenological issues related to the description of the structure function F_2 at low x we have also emphasised the role of studying the hadronic final state in deep inelastic scattering for probing the QCD pomeron. Finally let us point out that the recent experiments at HERA cover very broad range of Q^2 including the region of low and moderately large values of Q^2 . Analysis of the structure functions in this transition region is very interesting [87] and may help to understand possible relation (if any) between the soft and hard pomerons.

Acknowledgments

I thank the organizers of the School for organizing an excellent meeting. I thank Barbara Badelek, Krzysztof Golec-Biernat, Sabine Lang, Claire Lewis, Alan Martin and Peter Sutton for the very enjoyable research collaboration on problems presented in these lectures. This research has been supported in part by the Polish State Committee for Scientific Research grant 2 P03B 231 08 and the EU under contracts n0. CHRX-CT92-0004/CT93-357.

References

- [1] L.N. Gribov, E.M. Levin and M.G. Ryskin, Phys. Rep. **100** (1983) 1.
- [2] B. Badelek et al., Rev. Mod. Phys. **64** (1992) 927.
- [3] A.D. Martin, Acta. Phys. Polon, **B25** (1994) 265.
- [4] J. Kwieciński, Nucl. Phys. B (Proc. Suppl.) **39 B,C** (1995) 58.
- [5] A.J. Askew et al., Phys. Rev. **D47** (1993) 3775; Phys. Rev. **D49** (1994) 4402.
- [6] H1 collaboration: A. de Roeck et al., Proc. of the Workshop on DIS and QCD J., Paris, France, 24-28 April 1995, J.F. Laporte and Y. Sirois (Editors).

- [7] ZEUS collaboration: B. Foster, Proc. of the Workshop on DIS and QCD J., Paris, France, 24-28 April 1995, J.F. Laporte and Y. Sirois (Editors).
- [8] B. Badelek et al., J. Phys. **G22** (1996) 815.
- [9] M. Lancaster, J. Phys. **G22** (1996) 747.
- [10] H. Abramowicz, Rapporteur talk presented at the 28th International Conference on High Energy Physics, Warsaw, Poland, 25-31 July 1996.
- [11] E.A. Kuraev, L.N. Lipatov and V.S. Fadin, Zh. Eksp. Teor. Fiz. **72** (1977) 373 (Sov. Phys. JETP **45** (1977) 199); Ya. Ya. Balitzkij and L.N. Lipatov, Yad. Fiz. **28** (1978) 1597 (Sov. J. Nucl. Phys. **28** (1978) 822); J.B. Bronzan and R.L. Sugar, Phys. Rev. **D17** (1978) 585; T. Jaroszewicz, Acta. Phys. Polon. **B11** (1980) 965.
- [12] L.N. Lipatov, in "Perturbative QCD", edited by A.H. Mueller, (World Scientific, Singapore, 1989), p. 441.
- [13] P.D.B. Collins, "An Introduction to Regge Theory and High Energy Physics", Cambridge University Press, Cambridge, 1977.
- [14] A. Donnachie and P.V. Landshoff, Phys. Lett. **B296** (1992) 257.
- [15] A. Donnachie and P.V. Landshoff, Z. Phys. **C61** (1994) 161.
- [16] B.L. Ioffe, V.A. Khoze and L.N. Lipatov, "Hard Processes", North Holland, Amsterdam-Oxford-NewYork-Tokyo, 1984.
- [17] J. Ellis and M. Karliner, Phys. Lett. **B231** (1988) 72.
- [18] M. Ciafaloni, Nucl. Phys. **B296** (1988) 49.
- [19] A.D. Martin, J. Kwieciński and P.J. Sutton, Nucl. Phys. B (Proc. Suppl.) **A29** (1992) 67.
- [20] B. Andersson, G. Gustafson and J. Samuelsson, Z. Phys. **C71** (1996) 613 .
- [21] J. Kwieciński, A.D. Martin, P.J. Sutton, Z. Phys. **C71** (1996) 585.
- [22] J.C. Collins, P.V. Landshoff, Phys. Lett. **B276** (1992) 196.
- [23] J.F. McDermott, J.R. Forshaw and G.G. Ross, Phys. Lett. **B349** (1995) 189.
- [24] A.H. Mueller, Nucl. Phys., **B415** (1994) 373; A.H. Mueller and B. Patel, Nucl. Phys. **B425** (1994) 471; A.H. Mueller, Nucl. Phys. **B437** (1995) 107; Chen Zhang and A.H. Mueller, Nucl. Phys. **B451** (1995) 579.
- [25] V.S. Fadin, L.N. Lipatov, DESY preprint 96 - 020.
- [26] S. Catani, M. Ciafaloni and F. Hautmann, Phys. Lett. **B242** (1990) 97; Nucl. Phys. **B366** (1991) 657; J.C. Collins and R.K. Ellis, Nucl. Phys. **B 360** (1991) 3; S. Catani and F. Hautmann, Nucl. Phys. **B427** (1994) 475.
- [27] M. Ciafaloni, Phys. Lett. **356** (1995) 74.
- [28] J. Kwieciński, A.D. Martin, Phys. Lett. **B353** (1995) 123.

- [29] T. Jaroszewicz, Phys. Lett. **B116** (1982) 291.
- [30] R.K. Ellis, Z. Kunszt and E.M. Levin, Nucl. Phys. **B420** (1994) 517; Erratum-ibid. **B433** (1995) 498.
- [31] R.K. Ellis, F. Hautmann and B.R. Webber, Phys. Lett. **B348** (1995) 582.
- [32] R.D. Ball and S. Forte, Phys. Lett. **351** (1995) 313.
- [33] J.R. Forshaw, R.G. Roberts and R.S. Thorne, Phys. Lett. **B356** (1995) 79.
- [34] G. Camici and M. Ciafaloni, Florence preprint DFF 250/6/96 (hep-ph/9606427).
- [35] S. Catani, Florence preprint DFF 248/4/96 (hep-ph/9609263).
- [36] S. Catani, F. Fiorani and G. Marchesini, Phys. Lett. **B234** (1990) 339; Nucl. Phys. **B336** (1990) 18; G. Marchesini, in Proceedings of the Workshop "QCD at 200 TeV", Erice, Italy, 1990, edited by L. Cifarelli and Yu. L. Dokshitzer (Plenum Press, New York, 1992), p. 183; G. Marchesini, Nucl. Phys. **B445** (1995) 49.
- [37] J. Kwieciński, A.D. Martin, P.J. Sutton, Phys. Rev. **D52** (1995) 1445.
- [38] Yu.L. Dokshitzer et al., Rev. Mod. Phys. **60** (1988) 373.
- [39] J. Kwieciński, A.D. Martin and P.J. Sutton, Phys. Rev. **D53** (1996) 6094.
- [40] A.D. Martin, R.G. Roberts and W.J. Stirling, Phys. Rev. **D50** (1994) 6734; Phys. Lett. **354** (1995) 155.
- [41] M. Glück, E. Reya and A. Vogt, Z.Phys. **C67** (1995) 433.
- [42] A.D. Martin, R.G. Roberts and W.J. Stirling, Phys. Lett. **B387** (1996) 419.
- [43] A. de Rujula et al., Phys. Rev. **D10** (1974) 1649.
- [44] V.G. Gorshkov et al., Yad. Fiz. **6** (1967) 129 (Sov. J. Nucl. Phys. **6** (1968) 95); L.N. Lipatov, Zh. Eksp. Teor. Fiz. **54** (1968) 1520 (Sov. Phys. JETP **27** (1968) 814).
- [45] J. Kwieciński, Phys. Rev. **D26** (1982) 3293.
- [46] R. Kirschner and L.N. Lipatov, Nucl. Phys. **B213** (1983) 122; R. Kirschner, Z. Phys. **C67** (1995) 459.
- [47] B.I. Ermolaev, S.I. Manayenkov and M.G. Ryskin, Z.Phys. **C69** (1996) 259.
- [48] J. Bartels, B.I. Ermolaev and M.G. Ryskin, Z. Phys. **C70** (1996) 273.
- [49] J. Kwieciński, Acta Phys. Polon. **B27** (1996) 893.
- [50] C. Bourrely and J. Soffer, Phys. Rev. **D51** (1995) 2108; Nucl. Phys. **B445** (1995) 341; Marseille preprint CPT-95/P.3224.
- [51] M. Glück, E. Reya and W. Vogelsang, Phys. Lett. **B359** (1995) 201.
- [52] T. Gehrmann and W.J. Stirling, Phys. Lett. **B365** (1996) 347.
- [53] J. Blümlein and A. Vogt, DESY preprint 95-175.

- [54] J. Bartels, B.I. Ermolaev and M.G. Ryskin, DESY preprint 96 - 025. .
- [55] S.D. Bass, P.V. Landshoff, Phys. Lett. **B336** (1994) 537.
- [56] F.E. Close, R.G. Roberts, Phys. Lett. **B336** (1994) 257.
- [57] A.H. Mueller, J. Phys. **G17** (1991) 1443 .
- [58] J. Bartels, M. Loewe and A. DeRoeck, Z. Phys. **C54** (1992) 635 .
- [59] W.K.Tang, Phys. Lett. **B278** (1992) 363.
- [60] J. Kwieciński, A.D. Martin and P.J. Sutton, Phys. Rev. **D46** (1992) 921; Phys. Lett. **B287** (1992) 254.
- [61] J. Bartels et al., Phys. Lett. **B384** (1996) 300.
- [62] E. Mroczko, talk presented at the 28th International Conference on High Energy Physics, Warsaw, Poland, 25-31 July 1996.
- [63] J. Kwieciński, A.D. Martin, P.J. Sutton and K.Golec-Biernat, Phys. Rev. **D50** (1994) 217 ; K.Golec-Biernat, J. Kwieciński, A.D. Martin and P.J. Sutton, Phys. Lett. **B335** (1994) 220.
- [64] M. Kuhlen, Proc. of the Workshop on DIS and QCD, Paris, France, 14-28 April 1995, J.F. Laporte and Y. Sirois (editors).
- [65] V. del Duca, Phys. Rev. **D49** (1994) 4510.
- [66] W.J. Stirling, Nucl. Phys. **B423** (1994) 56.
- [67] J.R. Forshaw and R.G. Roberts, Phys. Lett. **B335** (1994) 494 .
- [68] A.J. Askew et al., Phys. Lett. **B338** (1994) 92. 1996.
- [69] J. Kwieciński, S.C. Lang, A.D. Martin, Phys. Rev. **D54** (1996) 1877.
- [70] J. Kwieciński, S.C. Lang, A.D. Martin, Preprint Univ. Durham DTP/96/62 (to be published in Phys. Rev. D).
- [71] J. Kwieciński, C.A.M. Lewis, A.D. Martin, Preprint Univ. Durham DTP/96/48 (to be published in Phys. Rev. D).
- [72] ZEUS Collaboration, M. Derrick et al., Phys. Lett. **B315** (1993) 481; **332** (1994) 228; **B338** (1994) 483.
- [73] H1 Collaboration, T. Ahmed et al., Nucl. Phys. **B 429** (1994) 477; Phys. Lett. **B348** (1995) 681.
- [74] A. Donnachie and P.V. Landshoff, Nucl. Phys. **B244** (1984) 322 ; **B267** (1986) 690.
- [75] A. Capella et al., Phys. Lett. **B343** (1995) 403 .
- [76] J.C. Collins et al., Phys. Rev. **D51** (1995) 3182 .
- [77] K. Golec - Biernat and J. Kwieciński, Phys. Lett. **B353** (1995) 329.

- [78] T. Gehrmann and W.J. Stirling, Z. Phys. **C70** (1996) 89.
- [79] A. Capella et al, Phys. Rev. **D53** (1996) 2309.
- [80] K. Golec-Biernat, J. Phillips, J. Phys. **G22**, (1996) 921.
- [81] N.N. Nikolaev and B.G. Zakharov, Z.Phys. **C53** (1992) 331; Jülich preprint KFA-IKP (TH) -1993 - 17; M. Genovesse, N.N. Nikolaev and B.G. Zakharov Jülich preprint KFA-IKP (TH)- 1994-307 (Torino preprint DFTT 42/94).
- [82] E. Levin and M. Wüsthoff Phys. Rev. **D50** (1994) 4306; J. Bartels, H. Lotter and M. Wüsthoff, DESY preprint 94-95.
- [83] K.Golec-Biernat, J. Kwieciński, INP Kraków preprint 1734/PH.
- [84] J. Phillips, talk presented at the 28th International Conference on High Energy Physics, Warsaw, Poland, 25-31 July 1996.
- [85] W. Buchmüller, Phys. Lett. **B353** (1995) 335 .
- [86] A. Edin, G. Ingelman and J. Rathsman, Proc. of the Workshop on DIS and QCD, Paris, France, 14-28 April 1995, J.F. Laporte and Y. Sirois (editors).
- [87] B. Badełek and J. Kwieciński, Rev. Mod. Phys. **68** (1996) 445 .

Figure Captions

1. The exponent λ_{BFKL} of the $x^{-\lambda_{BFKL}}$ behaviour of the gluon distribution obtained by solving the BFKL equation (a) with (continuous curve) and (b) without (dashed curve) the constraint $q^2 < Q_t^2 x'/x$ imposed, as a function of (fixed) $\bar{\alpha}_S \equiv 3\alpha_S/\pi$. The dashed curve is $\lambda_{BFKL} = \bar{\alpha}_S 4 \ln 2$. The dotted curve (c) is the value of the exponent that is obtained if we keep only the next-to-leading order modification due to the constraint $q^2 < Q_t^2 x'/x$. (From [21]).
2. The continuous and dashed curves correspond to the values of the proton structure function F_2 obtained from the R_1 and R_2 sets of partons (which have, respectively, QCD couplings corresponding to $\alpha_s(M_Z^2) = 0.113$ and 0.120) at twelve values of x chosen to be the most appropriate for the new HERA data. For display purposes we add $0.5(12 - i)$ to F_2 each time the value of x is decreased, where $i = 1, 12$. For comparison the dotted curves show the prediction obtained from the GRV set of partons [41]. The experimental data are assigned to the x value which is closest to the experimental x bin. (From [42]).
3. Diagrammatic representation of (a) a deep-inelastic + forward jet event, and (b) a deep-inelastic (x, Q^2) + forward identified photon ($x_\gamma, k_{\gamma T}$) event. (From [69]).
4. The Feynman diagrams describing the $gq \rightarrow \gamma q$ subprocess embodied in the DIS + γ diagram shown in Fig. 3b. (From [69]).
5. The cross section, $\langle \sigma \rangle$ in pb, for deep inelastic + photon events integrated over $\Delta x = 2 \times 10^{-4}$, $\Delta Q^2 = 10 \text{ GeV}^2$ bins which are accessible at HERA, and subject to various acceptance cuts. The x dependence is shown for three different ΔQ^2 bins, namely (20,30), (30,40) and (40,50) GeV^2 . The $\langle \sigma \rangle$ values are plotted at the central x value in each Δx

bin and joined by straight lines. The continuous curves show $\langle\sigma\rangle$ calculated with Φ_i determined from the BFKL equation, whereas the dashed curves are obtained just from the driving terms $\Phi_i^{(0)}$, i.e. from the quark box. For clarity a vertical line links the pair of curves belonging to the same ΔQ^2 bin. (From [69]).

6. Diagrammatic representation of (a) a deep inelastic + forward jet event, and (b) a deep inelastic (x, Q^2) + identified forward π^0 $(x_\pi, k_{\pi T})$ event. (From [70]).
7. The cross section, $\langle\sigma\rangle$ in pb, for deep inelastic + π^0 events integrated over bins of size $\Delta x = 2 \times 10^{-4}$, $\Delta Q^2 = 10 \text{ GeV}^2$ which are accessible at HERA for π^0 's with transverse momentum $3 < k_{\pi T} < 10 \text{ GeV}$ and subject to various acceptance cuts. The $\langle\sigma\rangle$ values are plotted at the central x value in each Δx bin and joined by straight lines. The x dependence is plotted for three different ΔQ^2 bins, namely (20,30), (30,40) and (40,50) GeV^2 . The continuous curves show $\langle\sigma\rangle$ calculated with Φ_i obtained from the BFKL equation. The corresponding $\langle\sigma\rangle$ values calculated neglecting soft gluon resummation and just using the quark box approximation $\Phi_i = \Phi_i^{(0)}$ are plotted as dashed curves. For clarity a dotted vertical lines joins each pair of curves belonging to the same ΔQ^2 bin. (From [70]).
8. The decomposition of the proton structure function $F_2(x, Q^2)$ into contributions coming from different numbers of resolved gluon jets for experimentally accessible values of the resolution parameter $\mu = 3.5$ and 6 GeV . The decomposition is shown as a function of x for $Q^2 = 10 \text{ GeV}^2$. (From [71]).

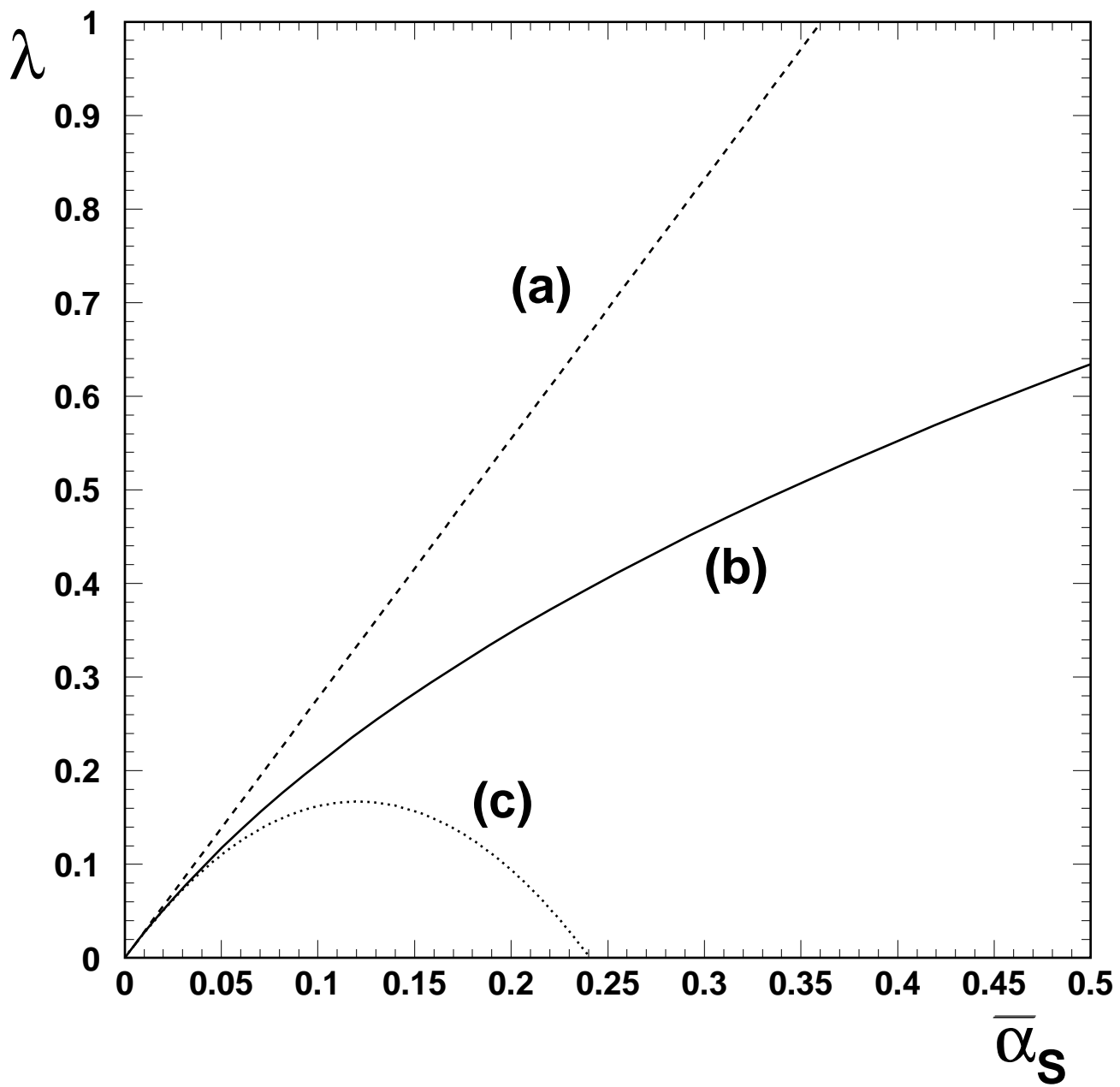


Fig. 1

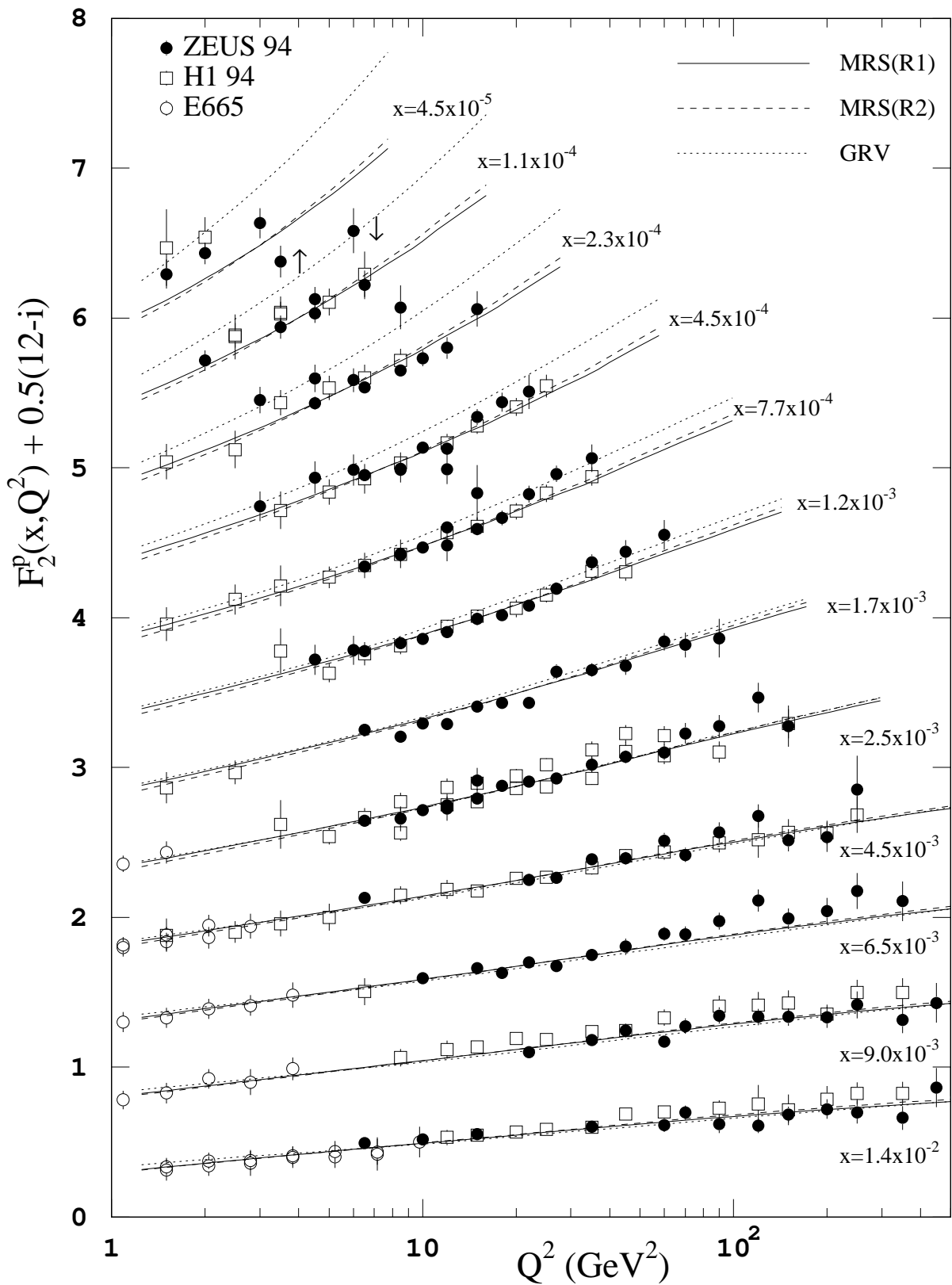
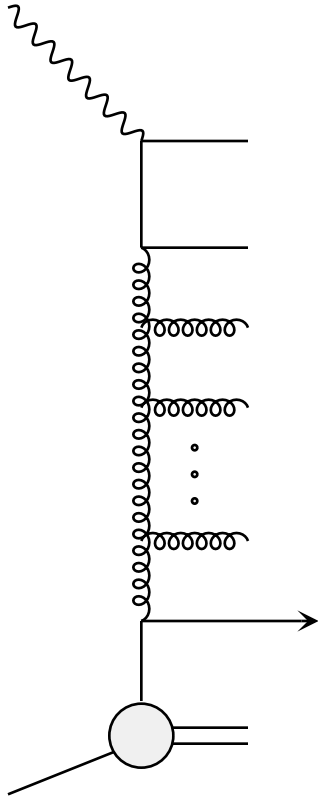


Fig. 2

(a) DIS + jet



(b) DIS + γ

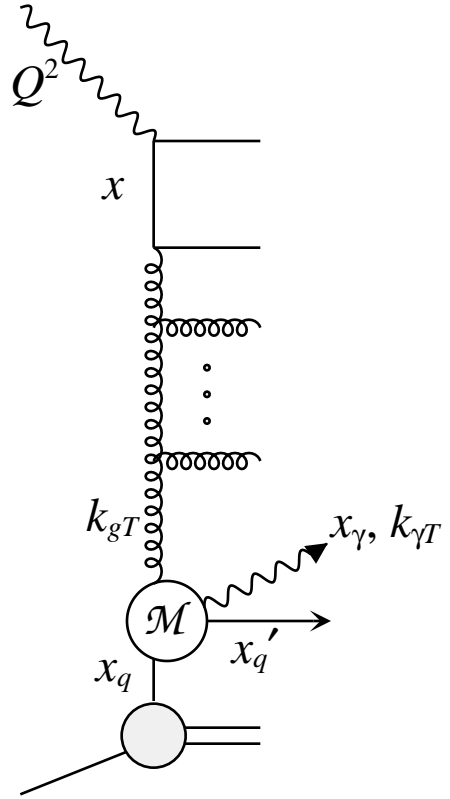


Fig.3

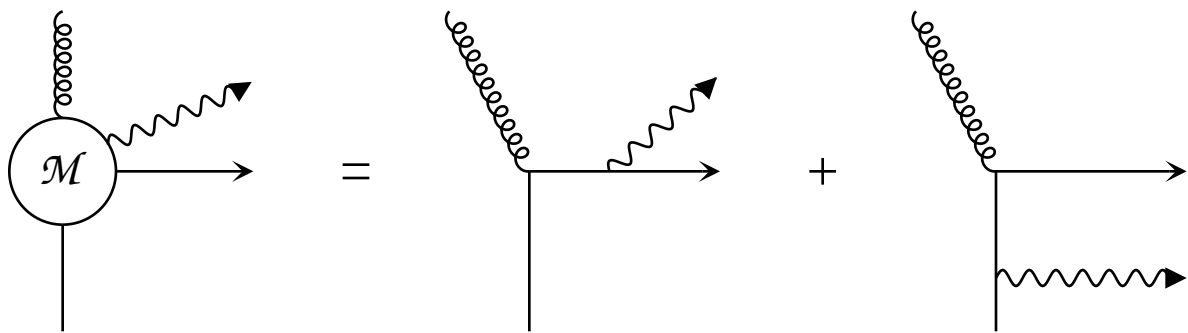


Fig.4

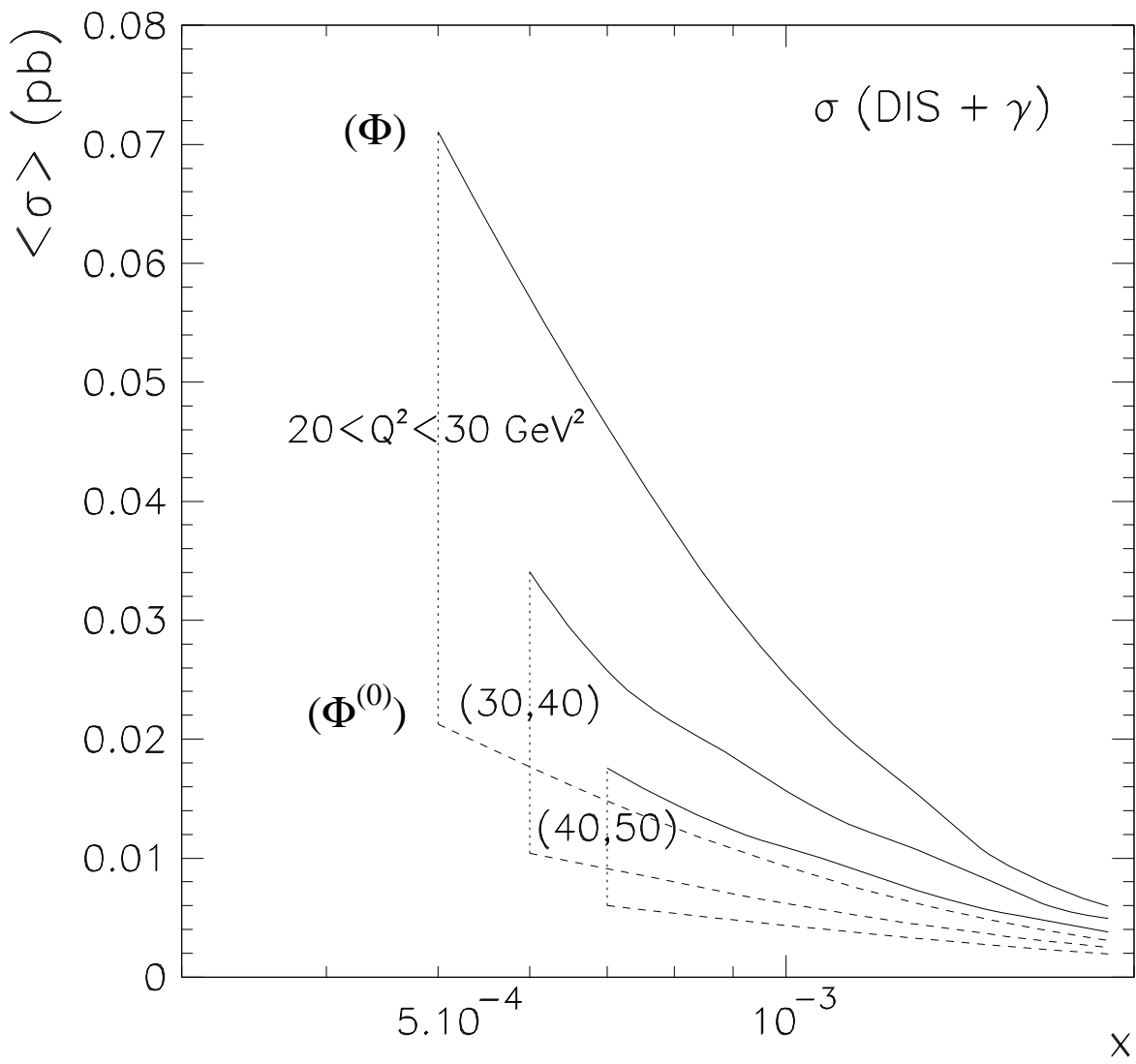
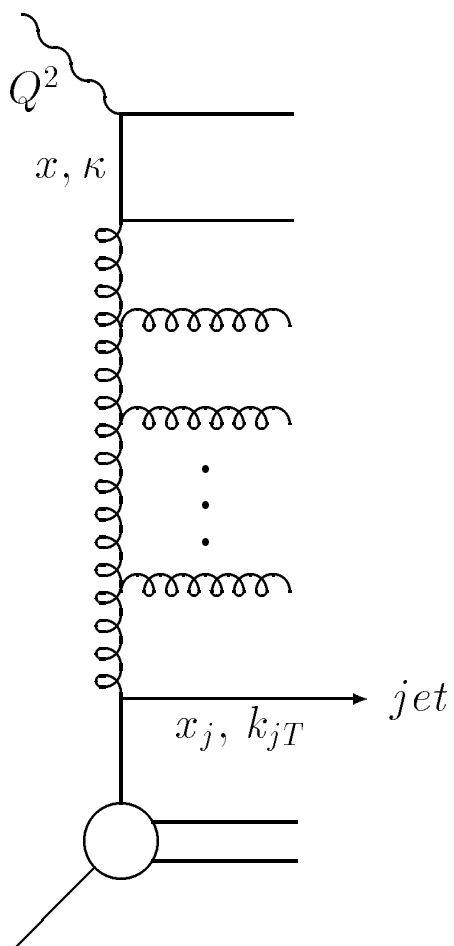


Fig.5

(a) DIS + jet



(b) DIS + π^0

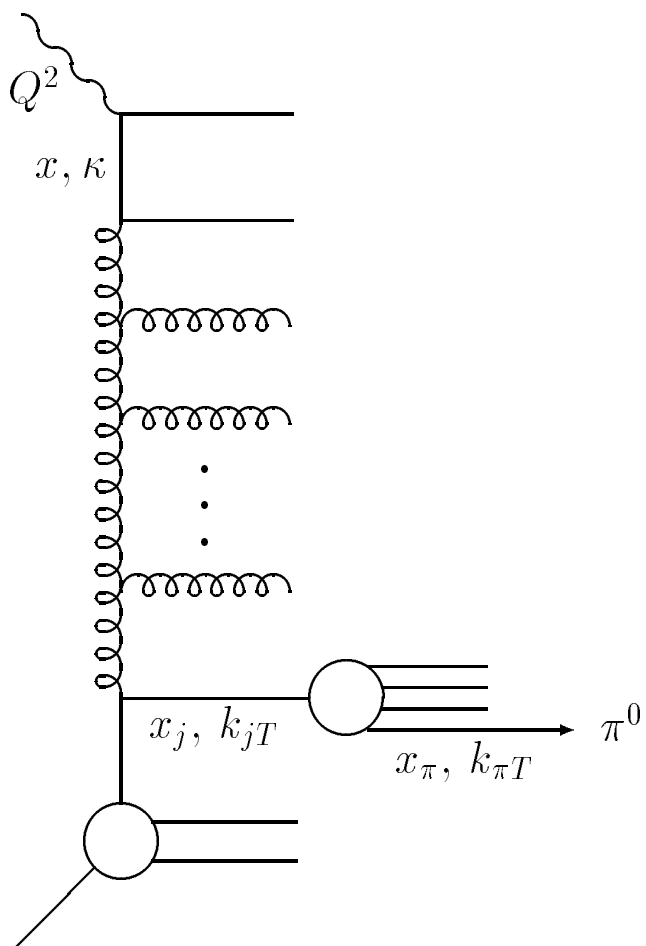


Fig. (

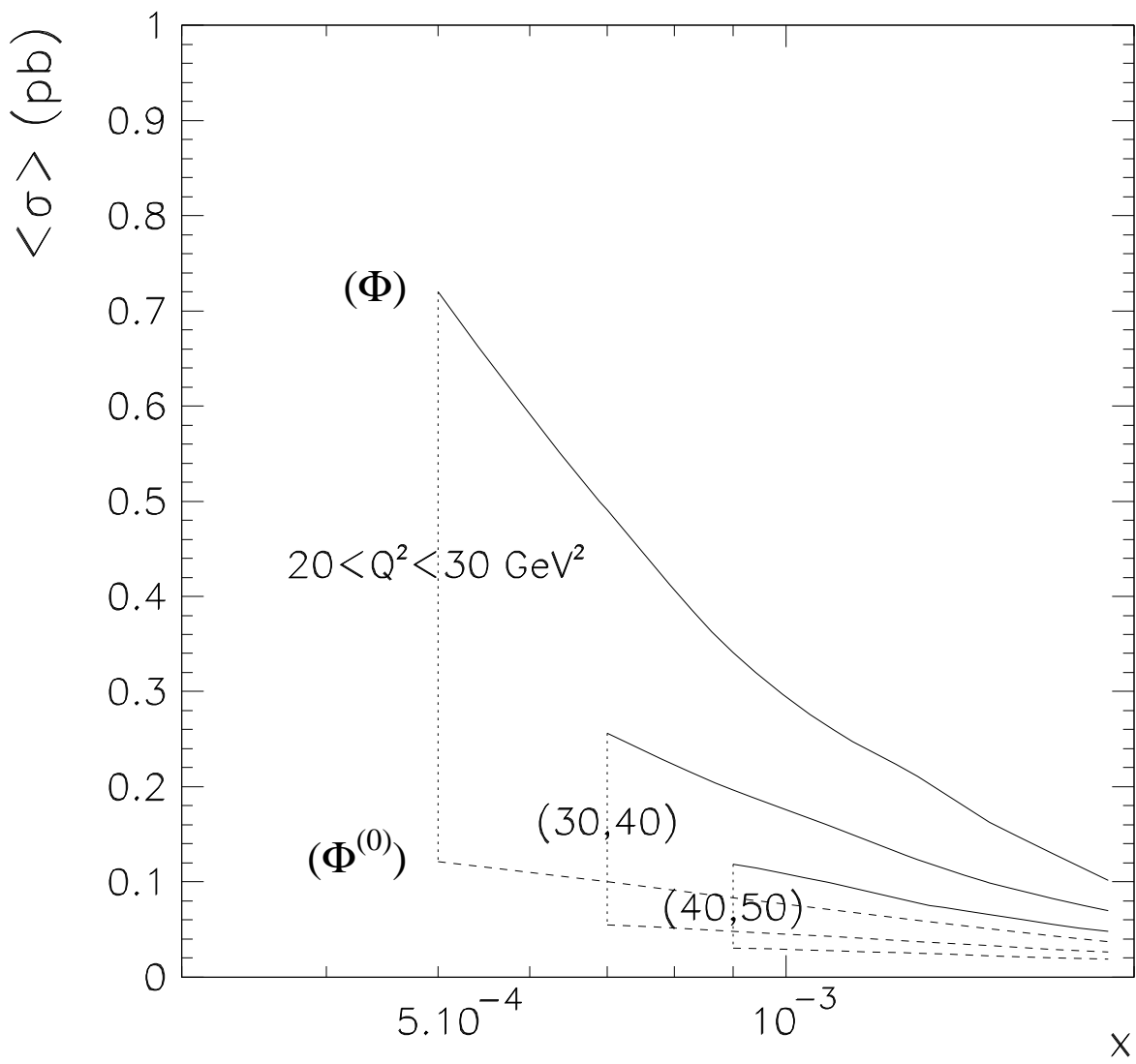


Fig.7

fig. 8

